Vol 15 No 11, November 2006
1009-1963/2006/15(11)/2571-07
Chinese Physics
© 2006 Chin. Phys. Soc.
and IOP Publishing Ltd

Partial wave scattering cross sections for He–HBr collision*

Yu Chun-Ri(余春日)[a)b)c)†], Feng Er-Yin(凤尔银)[b)],
Wang Rong-Kai(汪荣凯)[c)d)], and Yang Xiang-Dong(杨向东)[c)]

[a)] *School of Physics & Electric Engineering, Anqing Teachers College, Anqing* 246011, *China*
[b)] *Department of Physics, Anhui Normal University, Wuhu* 241000, *China*
[c)] *Institute of Atomic and Molecular Physics, Sichuan University, Chengdu* 610065, *China*
[d)] *School of Physics and Chemistry, Guizhou Normal University, Guiyang* 550001, *China*

(Received 25 May 2006; revised manuscript received 7 August 2006)

A new anisotropic potential is fitted to *ab initio* data. The close-coupling approach is utilized to calculate state-to-state rotational excitation partial wave cross sections for elastic and inelastic collisions of He atom with HBr molecule based on the fitted potential. The calculation is performed separately at the incident energies: 75, 100 and 200 meV.The tendency of the elastic and inelastic rotational excitation partial wave cross sections varying with total angular quantum number J is obtained.

Keywords: close-coupling approach, partial wave cross sections, He–BrH complex
PACC: 3440, 3430, 3450E

1. Introduction

The inelastic vibrational–rotational excitation between atom and molecule plays an important role in a great variety of physical processes, such as gas phase relaxation, gas phase reaction, energy transfer in chemical laser, thermal scattering in mixture gases, and cooling process in planetary space. It can provide a great deal of reference information for many branches of physics and chemistry, for example, plasma physics, laser physics, astrophysics, matter structure and chemical reaction dynamics.[1−3]

There exists a vast literature dealing with the interaction and dynamics between rare gas atom and hydrogen halide molecule.[4−7] However, it is inconvenient to obtain the scattering experimental data because of the strong causticity of hydrogen halide molecules, which is harmful to experimental apparatus. Thus it is especially important to theoretically investigate the vibrational and rotational excitations and obtain the scattering cross sections for the collisions between atom and molecule. In this paper, a new anisotropic potential is fitted to *ab initio* data. The close-coupling method is used to calculate the elastic and inelastic partial scattering cross sections for a He–HBr collision system at different collision energies. The tendency of the elastic and inelastic partial wave cross section varying with total angular quantum number J is obtained. We believe that the results are helpful for the scattering experiments and theoretical study of pressure broadening cross sections of spectrum lines.

2. Close-coupling approach

According to the close-coupling approach,[8] the differential cross-section (DCS) for the collision process between an atom (A) and a diatomic molecule (BC): A+BC (ν_α, j_α) → A+BC(ν_β, j_β) is given by

$$\frac{\mathrm{d}\sigma_{v_\alpha j_\alpha \to v_\beta j_\beta}}{\mathrm{d}\,\Omega} = \frac{1}{(2j_\alpha+1)} \times \frac{k_\beta}{k_\alpha} \sum_{M_\alpha M_\beta} |f_{v_\beta j_\beta M_\beta, v_\alpha j_\alpha M_\alpha}(\theta,\phi)|^2, \quad (1)$$

*Project supported by the National Natural Science Foundation of China (Grant Nos 10574096,10676025) and the Natural Science Foundation of Education Bureau of Anhui Province, China.
†E-mail: cryu@aqtc.edu.cn, cryu2@sina.com

where ν is the molecular vibrational quantum number, j is the rotational quantum number, M is the quantum number of projection of rotational quantum number onto a spaced-fixed axis, and k represents the wavevector,

The scattering amplitude from the initial state $(v_\alpha j_\alpha M_\alpha)$ to the final state$(v_\beta j_\beta M_\beta)$ is

$$f_{v_\beta j_\beta M_\beta, v_\alpha j_\alpha M_\alpha}(\theta,\phi) = \Big(\frac{4\pi}{k_\alpha k_\beta}\Big)^{1/2} \times \sum_{l_\beta} [2l_\beta+1]^{1/2} A_{l_\beta}(v_\alpha j_\alpha M_\alpha \to v_\beta j_\beta M_\beta) Y_{l_\beta M_\alpha \to M_\beta}(\theta,\phi) \tag{2}$$

with

$$A_{l_\beta}(v_\alpha j_\alpha M_\alpha \to v_\beta j_\beta M_\beta) = \sum_J \langle l_\beta M_\alpha - M_\beta j_\beta M_\beta | J M_\alpha \rangle T^J_{v_\alpha j_\alpha l_\alpha, v_\beta j_\beta M_\beta}, \tag{3}$$

where l is the quantum number of orbital angular momentum, J denotes the quantum number of total angular momentum, $Y_{l_\beta M_\alpha \to M_\beta}(\theta,\phi)$ is the spherical harmonics and $T^J_{v_\alpha j_\alpha l_\alpha, v_\beta j_\beta M_\beta}$ is the transition matrix element.

The total partial cross section (PCS) for the collision procedure A+BC(ν_α, $j_\alpha = 0$) $\to$ A+BC(ν_β, j_β) is given by

$$\sigma^J_{\nu_\alpha j_\alpha \to \nu_\beta j_\beta} = \frac{1}{2j_\alpha+1} \times \frac{4\pi}{K^2_\alpha} \sum_{l_\beta M_\alpha} (2l_\beta+1) |T^J_{v_\alpha j_\alpha l_\alpha, v_\beta j_\beta M_\beta}|^2 . \tag{4}$$

3. Results and discussion

3.1. The anisotropic potential for He–HBr interaction

As usual, we expand the potential energy surface of He–HBr as

$$V(R,r,\theta) = \sum_\lambda V_\lambda(R,r) P_\lambda(\cos\theta),$$
$$\lambda = 0,1,2,\ldots \tag{5}$$

where $P_\lambda(\cos\theta)$ denotes the Legendre polynomial, $\cos\theta = \hat{\boldsymbol{R}} \bullet \hat{\boldsymbol{r}}$ is shown in Fig.1, where $\hat{\boldsymbol{R}}$ and $\hat{\boldsymbol{r}}$ are unit vectors. Here, we discuss only the rotation excitation, the r is fixed at its equilibrium position. Then, the radial potential function is given by the Barker potential-type[9]

$$V_\lambda(R) = \varepsilon\Big[\exp(\alpha(1-x)) \sum_{n=0}^{3} A_n (x-1)^n - \frac{C_6}{x^6+\delta} - \frac{C_8}{x^8+\delta}\Big], \tag{6}$$

where $x = R/R_m$, ε is the depth of potential well, R_m is the position of potential well, α, A_0, A_1, A_2, A_3, C_6, C_8 and δ are the fitted parameters, which are shown in Table 1. We plot the fitted radial potential curves $V_\lambda(\lambda = 0,1,2,3,4)$ in Fig.2.

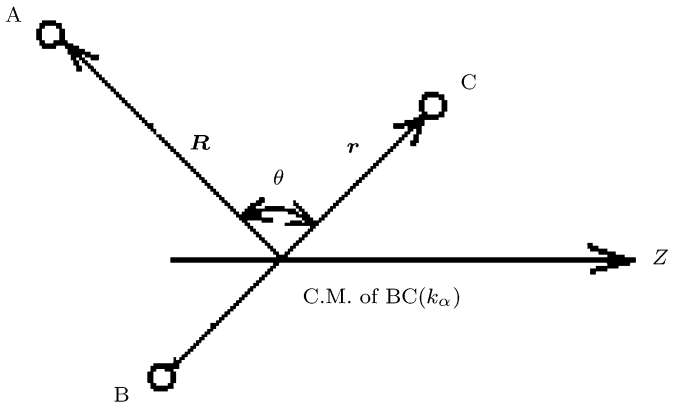


Fig.1. Geometry of the scattering between an atom (A) and a diatomic molecule (BC).

Table 1. The fitted potential parameters for He–HBr system

Coeffient	ε/ meV	R_m/nm	α	A_0	A_1	A_2	A_3	C_6	C_8	δ
V_0	2.1899	0.3958	14.3390	−0.4637	−5.1226	−9.3909	−4.4808	3.0650	−2.5266	0.0200
V_1	0.4369	0.4184	15.6464	−3.6990	−22.4811	−42.1387	−25.7093	7.4160	−10.2372	0.0273
V_2	0.9819	0.3724	7.9424	−20.1993	−30.9991	−18.8548	−206.2509	−7.5726	−13.2401	0.0818
V_3	0.2220	0.4311	10.1383	8.4149	6.5421	35.1262	0.0001	−4.6934	14.8549	0.0754
V_4	0.1013	0.4366	15.3937	−1.6382	−20.7189	−45.7622	−35.9497	0.0105	0.0067	−0.0791

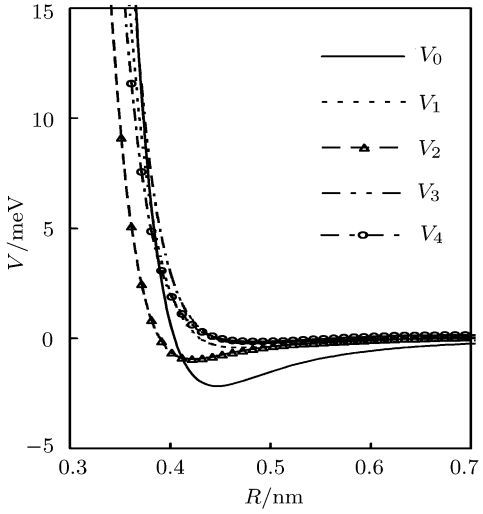


Fig.2. The radial potential curves of the BFW model.

Figure 3 shows a comparison between the spherical symmetry term V_0 of our fitted potential and the exponential-spline-Morse–Spline–van der Waals (ESMSV) potential.[10] The agreement confirms the reliability of our fitted potential.

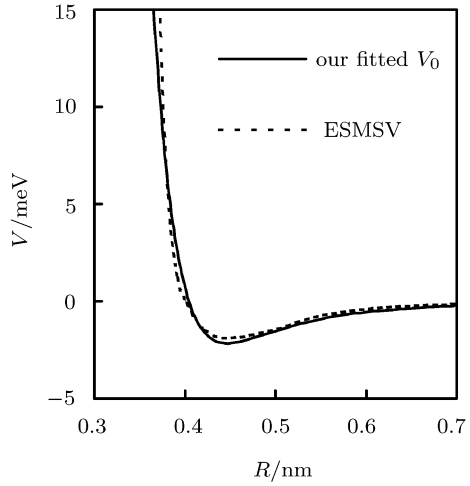


Fig.3. Comparison of the spherical symmetry term V_0 of the BFW with ESMSV potential.

3.2. The partial wave cross sections for He–HBr collision

We have calculated the partial wave cross sections for He–HBr elastic collisions $j = 0 \to j' = 0$ and the state-to-state excitation partial wave cross sections of rotation $j = 0 \to j' = 1 - 13$ at the incident energies: 75, 100 and 200 meV, separately. The results are shown in Figs.4–14. The energies of the vibrational and rotational excitations for HBr molecules are as follows:

$$
\begin{aligned}
&E_{00-01} = 2.1 \text{ meV}, \quad E_{00-02} = 6.2 \text{ meV},\\
&E_{00-03} = 12.4 \text{ meV}, \quad E_{00-04} = 20.7 \text{ meV},\\
&E_{00-05} = 31.0 \text{ meV}, \quad E_{00-06} = 43.4 \text{ meV},\\
&E_{00-07} = 57.8 \text{ meV}, \quad E_{00-08} = 74.3 \text{ meV},\\
&E_{00-09} = 92.8 \text{ meV}, \quad E_{00-10} = 113.3 \text{ meV},\\
&E_{00-11} = 135.9 \text{ meV}, \quad E_{00-12} = 160.4 \text{ meV},\\
&E_{00-13} = 187.0 \text{ meV}, \quad E_{00-14} = 215.5 \text{ meV}\,.
\end{aligned}
$$

It can be seen from the above data that when the incident energy E is 75 meV the excitation must include all states lower than $j' = 8$, and when incident energies are 100 and 200 meV the states which j' being 9 and 13 are excited respectively.

The calculated partial wave number is 110 for each of incident energies. We assume that the partial wave is convergent when the value of partial wave cross section reaches $10^{-4}a_0^2$, where a_0 is Born radius. Figure 4 shows the variation of the partial wave cross sections for He–HBr elastic collisions (00–00) with the increase of rotational quantum number J. We can see from the figure that for each given incident energy E, the elastic partial wave cross section keeps oscillatory with the increase of quantum number J, the oscillating amplitude increases until it reaches a maximum finally, and after that it approaches zero rapidly. As the incident energy increases, the position of oscillation maximum gradually shifts towards large values of J, while the amplitude decreases. In addition, the cross section slowly converges with the increase of the

incident energy. For example,

$$E = 75 \text{ meV}, \quad J_{\text{peak}} = 32,$$
$$\sigma_{00-00}^{\text{peak}} = 15.6a_0^2, \quad J' = 78;$$
$$E = 100 \text{ meV}, \quad J_{\text{peak}} = 38,$$
$$\sigma_{00-00}^{\text{peak}} = 13.0a_0^2, \quad J' = 89;$$
$$E = 200 \text{ meV}, \quad J_{\text{peak}} = 54,$$
$$\sigma_{00-00}^{\text{peak}} = 8.94a_0^2, \quad J' = 107.$$

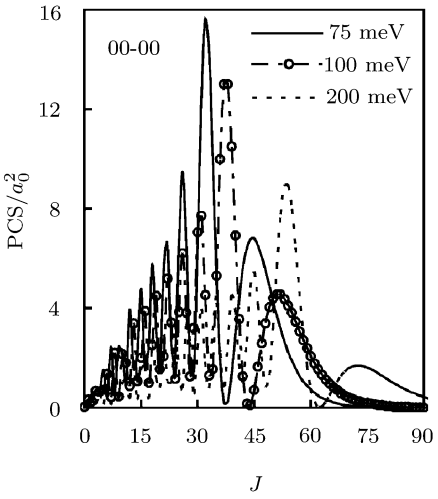


Fig.4. The elastic PCS at different energies.

Another feature in Fig.4 is tail effect. With the increase of the incident energy, the tail effect becomes weaker and weaker as the corresponding quantum number J increases. For instance,

$$E = 75 \text{ meV}, \quad J = 45, \quad \sigma_{\text{tail}}^{\max} = 6.80a_0^2;$$
$$E = 100 \text{ meV}, \quad J = 51, \quad \sigma_{\text{tail}}^{\max} = 4.55a_0^2;$$
$$E = 200 \text{ meV}, \quad J = 73, \quad \sigma_{\text{tail}}^{\max} = 1.69a_0^2.$$

This phenomenon can be explained as follows: the lower the incident energy is, the more prominent the wave property of the scattering particle is. When the angular quantum of the incident particle is large enough, the particle cannot interact with the scattering potential field from the viewpoint of classical scattering, but the particle can still be scattered by the potential field because of quantum effect.

Figures 5–14 show the state-to-state inelastic rotational excitation PCS for He–HBr collisions at different energies. From the figures, it can be seen easily that there exists a tail effect for the rotational transitions of 00–01, 00–02, 00–03, but no tail effect for the higher rotational transitions of 00–04, 00–05 and so on. Therefore, it indicates that the tail effect is present only in lower excited states but not in higher excited states.

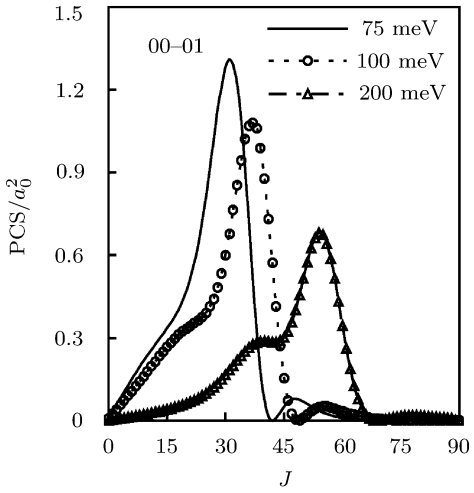


Fig.5. The rotational excitation PCS at different energies.

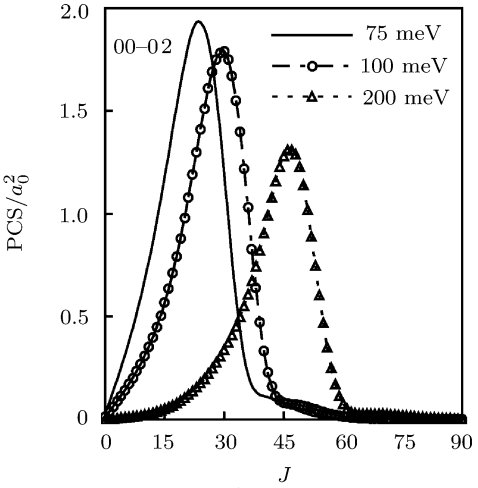


Fig.6. The rotational excitation PCS at different energies.

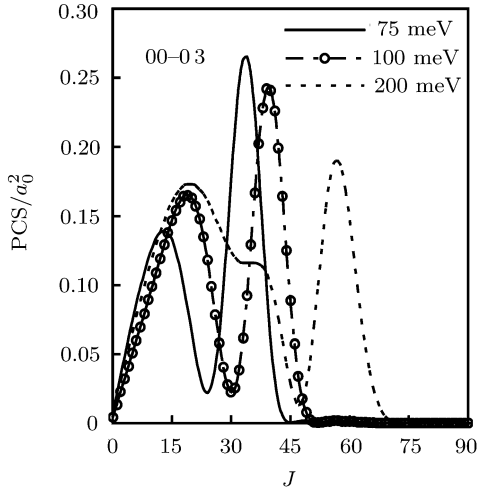


Fig.7. The rotational excitation PCS at different energies.

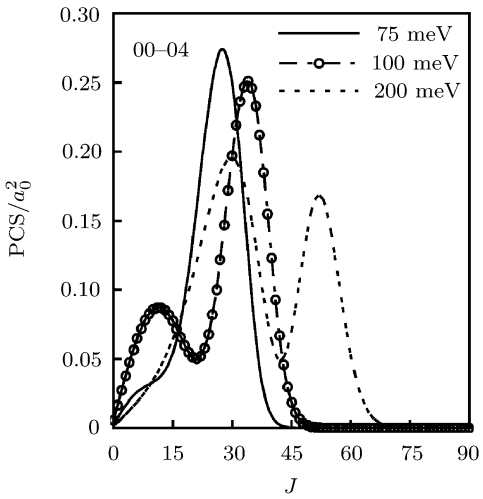


Fig.8. The rotational excitation PCS at different energies.

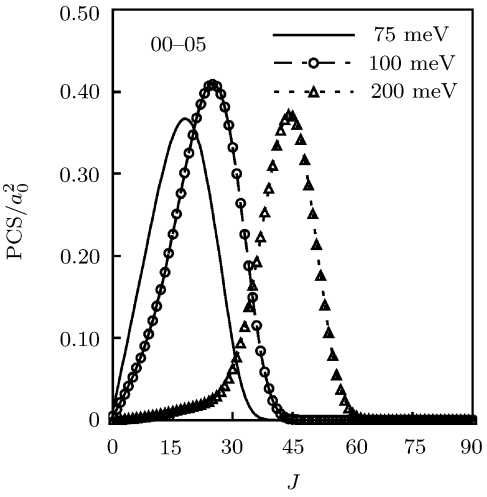


Fig.9. The rotational excitation PCS at different energies.

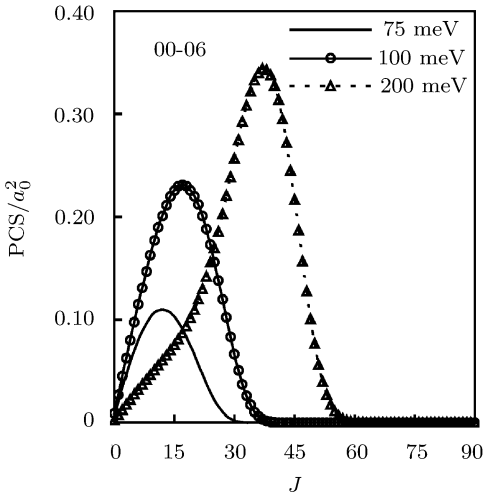


Fig.10. The rotational excitation PCS at different energies.

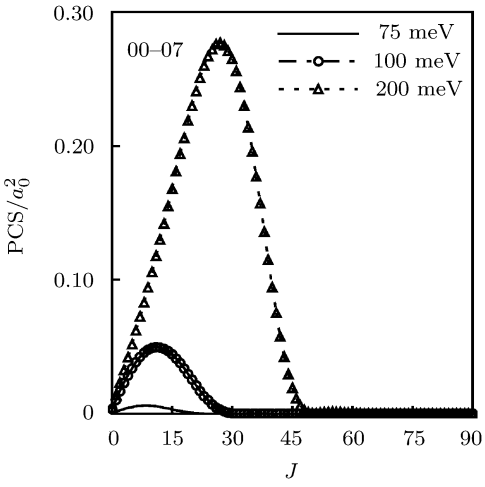


Fig.11. The rotational excitation PCS at different energies.

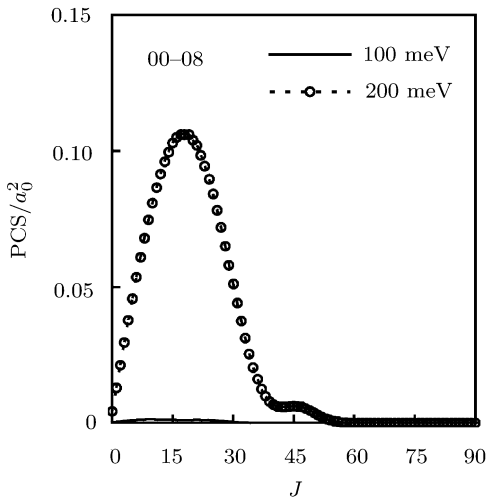


Fig.12. The rotational excitation PCS at different energies.

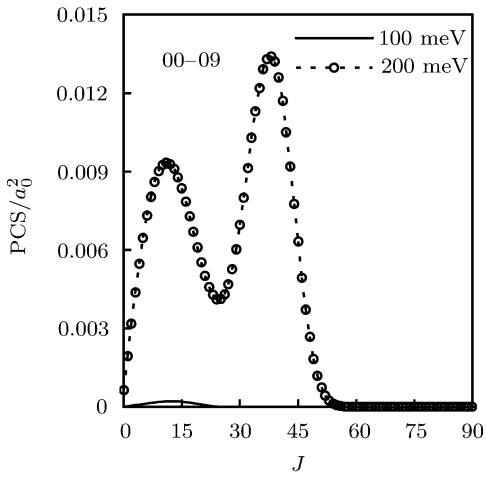


Fig.13. The rotational excitation PCS at different energies.

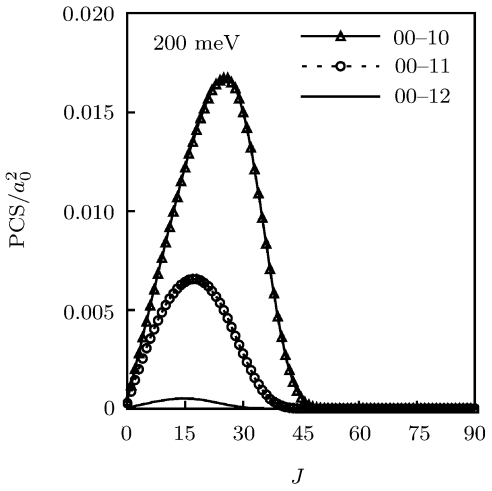


Fig.14. The rotational excitation PCS at 200 meV.

Table 2 displays the peak value of the partial wave cross section for each inelastic excitation, corresponding partial number J and the converged partial number J' for the He–HBr system. From these figures and tables above, it can be seen that the excitation partial wave cross sections converge faster than that of elastic partial wave cross sections. The excitation partial wave cross sections converge more rapidly for the higher excited states, but more slowly for the higher incident energies. In addition, for different incident energies, the variations of the state-to-state rotational excitation partial wave cross sections are similar to each other. For each of the three incident energies considered here, the peak value of the partial wave cross section is present in the excitation of 00–02, another local maximum occurs in the excitation of 00–05. The tendency of the variation in the excitation partial wave cross sections for He–HBr collisions is in accord with that for He–HCl collisions.[4]

Table 2. The peak value of the partial wave cross section for each excitation, corresponding partial number J and convergent partial number J' for He–HBr system.

	75 meV			100 meV			200 meV		
	PCS/ a_0^2	J	J'	PCS/ a_0^2	J	J'	PCS/ a_0^2	J	J'
00-00	15.6	32	78	13.0	38	89	8.94	54	107
00–01	1.31	31	69	1.08	37	78	0.681	54	94
00–02	1.93	24	66	1.79	30	75	1.31	47	89
00–03	0.265	34	54	0.242	39	62	0.190	57	72
00–04	0.273	28	44	0.251	34	50	0.168	52	70
00–05	0.367	18	39	0.409	25	45	0.372	44	64
00–06	0.110	12	31	0.231	17	39	0.344	37	60
00–07	0.00597	9	20	0.0497	11	29	0.277	27	58
00–08				0.00124	10	25	0.106	19	54
00–09							0.0134	38	51
00–10							0.0167	26	44
00–11							0.00655	17	40

4. Conclusions

Based on the above discussion for a He–HBr collision system, we can draw some conclusions as follows:

(1) The tail effect is present only in the process of elastic collision and lower excited state transitions, and the higher the energy of the incident particle is, the weaker the tail effect is.

(2) The excitation partial wave cross sections converge faster than the elastic partial wave cross sections. With the increase of incident energy, the excitation partial wave cross sections converge more rapidly for the higher excited states, and more slowly for the higher incident energies.

(3) For each of the three incident energies considered here, the peak value of the partial wave cross section is present in the excitation of 00–02, another local maximum appears in the excitation of 00–05.

References

[1] Buck U 1982 *Faraday Discussion Chem. Soc.* **73** 187

[2] Monchick L, Munn R J and Mason E A 1966 *J. Chem. Phys.* **45** 3051

[3] Yang X D, Zhang J Y and Jing F J 1998 *Chin. Phys. Lett.* **15** 19

[4] Yu C R, Huang S Z, Feng E Y, Wang R K, Cheng X L and Yang X D 2006 *Acta Phys. Sin.* **55** 2215 (in Chinese)

[5] Sun G H, Yang X D, Zhu J and Wang C X 2002 *Chin. Phys.* **11** 910

[6] Moszynski R, Wormer P E.S, Jeziorski B and Avoird A 1994 *J. Chem. Phys.* **101** 2811

[7] Zhang Y, Shi H Y and Wang W Z 2002 *Acta Chim. Sin.* **60** 1011 (in Chinese)

[8] Choi B H and Tang K T 1975 *J. Chem. Phys.* **63** 1775

[9] Yu C R 2006 *J. At. Mol. Phys.* **23** 310 (in Chinese)

[10] Held W D, Piper E, Ringer G and Toennies J P 1980 *Chem. Phys. Lett.* **75** 260